

Dodecanogram (DDG): Advancing EEG technology with a high-frequency brain activity measurement device

P. Singh¹, J. S. Manna^{1,2}, P. Dey^{1,3}, S. Sarkar⁴, A. Pattanayaka^{4,5}, S. Nag⁴, S. Pramanik⁶, K. Saxena^{1,7}, S. D. Krishnananda⁷, T. Dutta⁴ & A. Bandyopadhyay^{1*}

¹International Center for Materials and Nanoarchitectonics (MANA), NIMS, 1-2-1 Sengen, Tsukuba, Ibaraki-3050047, Japan.

²Department Electronics and Electrical Communication Engineering, IIT Kharagpur, 721302 West Bengal, India.

³Cancer Biology Laboratory and DBT-AIST International Centre for Translational and Environmental Research (DAICENTER), Department of Biosciences and Bioengineering, Indian Institute of Technology Guwahati, Assam 781039, India

⁴Organizational Behavior and Human Resource Management, Indian Institute of Management, Ranchi, India-834008.

⁵School of Commerce, XIM University, Plot No 12(A); Nijigada, Kurki, Harirajpur, Odisha, 752050, India.

⁶Amity School of Applied Science, Amity University Rajasthan, Kant Kalwar, NH-11C, Jaipur Delhi Highway, Jaipur, Rajasthan 303007, India.

⁷Microwave Physics Laboratory, Department of Physics and Computer Science, Dayalbag Educational Institute, Agra, Uttar Pradesh 282005, India.

*Correspondence: anirban.bandyopadhyay@gmail.com

DOI: <https://doi.org/10.56280/1600841751>



This article is an open access article distributed under the terms and conditions of the Creative Commons Attributions (CC BY) license (<https://creativecommons.org/licenses/by/4.0/>)

Received: 22 November 2023

Accepted: 27 November 2023

Online Published: 12 December 2023

Abstract

EEG measures electric potential changes in the scalp. Even though it has been associated with human thoughts, there has been no direct evidence. The problem with EEG is that it measures variations in current or electric potential in the millisecond time domain, where muscle movement strongly affects the readings. The millisecond time domain is equivalent to the kHz resonance signal generated by any dielectric resonator, and every single cell membrane resonates in this time range. So, the measurement of EEG could come simply from the skin and not from the brain. Therefore, we have advanced EEG technology with the dodecanogram (DDG), which reveals 12 frequency bands or 12 discrete time regions where brain activities are most significant. We measure brain activity using a stream of pulses and a logic analyzer that counts ultra-short pulses needed to emulate brain scalp potential changes. We have created another version of DDG where, using an array of RLC (resistor-inductor-capacitor) resonators, we sense the ultra-low-power electromagnetic radiation from different locations on the brain's surface. Since we measure signals from Hz to THz, covering 12 orders of time ranges as a property of dielectric resonance, unlike EEG, there is a high probability that the DDG signal may truly originate from the brain. We have monitored DDG on an artificial organic brain replica 24/7 for over a year and on multiple human subjects, before and after meditation and concluded that most cognitive, perceptive and emotional bursts occur around 200-700 nanoseconds, not milliseconds, as it was believed for 150 years of EEG era.

Keywords: Dodecanogram (DDG), Electroencephalogram (EEG), electromagnetic, human subject, cognition, time crystal, artificial brain, synchronization, desynchronization.

1. Introduction

EEG (electroencephalography) is a widely used technique to measure the electrical activity of the brain. Electroencephalogram (EEG) is a pivotal tool in neuroscience, facilitating the study of brain activity and behavior (Jiang *et al.*, 2019). It entails the recording of brain electrical activity over a specific timeframe (Joshi & Shakya, 2017). However, it is important to note that EEG does not directly measure the real brain signal. Instead, it measures the electric potential from the surface of the scalp (Hughes & John, 1999). This means that EEG signals are influenced by various factors, such as the conductivity of the tissues between the brain and the electrodes, the distance between the brain and the electrodes, and the filtering and processing of the signals (Darvas *et al.*, 2016).

While EEG has a broad range of applications, it is inherently limited in its capacity to monitor brain activity within a restricted frequency range, 1Hz to 300Hz (Vanhatalo *et al.*, 2005; Niedermeyer, 2005). EEG recordings have relied on wet electrodes that necessitate the application of conductive gel for optimal scalp-skin electrical connectivity, essentially measuring brain activities indirectly. EEG has been repeatedly claimed to furnish insights into the brain electrical activity, enabling the identification of anomalous wave patterns or energy characteristics associated with brain function (Siddiqui *et al.*, 2020; Buzsáki, & Draguhn, 2004). EEG, discovered in the 19th century (1875), has transformed the background of brain research and the investigation of neural activity (Berger, 1929). Nevertheless, an in-depth study of its data analysis exposes limitations, necessitating a call for reform. One of the limitations of EEG is that it filters data and removes unwanted and abrupt peaks, which may not necessarily be incorrect steps (Hughes & John, 1999). Commercial EEG signal processors often perform automatic signal processing, but it is important to note that this processing may not always be accurate. Therefore, it is crucial to critically evaluate the processed EEG data and consider the potential limitations and artifacts introduced during the signal processing.

Advances in electrode technology and the application of machine learning techniques have significantly

enhanced EEG's capabilities, enabling more precise diagnosis and monitoring (Fiedler *et al.*, 2015; Benbadis, 2019). However, a primary limitation of EEG lies in its inability to monitor brain activity across a broad frequency range (Nunez, 2006).

While EEG provides valuable insights into brain activity, it has limitations in terms of spatial resolution. EEG electrodes can only measure the electrical activity of superficial brain structures with variable resolution and localization accuracy (Darvas *et al.*, 2016; Kurkin *et al.* 2020). Invasive microelectrode recordings, on the other hand, can measure neuronal spikes that are commonly considered inaccessible through standard surface EEG (Teleńczuk *et al.*, 2011). Therefore, combining EEG with other techniques, such as invasive recordings or neuroimaging methods like fMRI, can provide a more comprehensive understanding of brain activity.

High-frequency EEG is an area of growing interest in research. While most EEG studies focus on lower frequency bands, high-frequency EEG has the potential to provide valuable information about brain function (Teleńczuk *et al.*, 2011). However, there is a limited number of high-frequency EEG studies that have been performed, and further research is needed to fully understand its implications and applications. EEG measures the electric potential from the surface of the scalp and does not directly measure the real brain signal. The automatic signal processing by extensive filtering and normalization performed by commercial EEG signal processors may not always be accurate. EEG has limitations in terms of spatial resolution, but it can be complemented with other techniques to provide a more comprehensive understanding of brain activity. High-frequency EEG is an emerging area of research that requires further investigation to fully explore its potential.

To address these limitations, we have introduced an improved EEG device for high-frequency brain scanning: Dodecanogram (DDG), featuring 34 electrodes, each employing a Yagi antenna to sense the brain signals from 6THz to 1 milliHz frequency domain (Fig.1a &b) and replicated the biological human brain structure, including the use of similar dielectric materials and the replication of all components of the brain-body neural network.

In **Figure 1a**, we show that an extensive amount of research has been performed to understand the origin of EEG. The origin of EEG signals has been a subject of extensive research, particularly in understanding how the signal, which is limited to milliseconds, can be generated from synaptic junctions, and leave a projection on the brain scalp. The use of EEG and fMRI simultaneously has provided valuable insights into this phenomenon. Studies have shown that the simultaneous acquisition of EEG with fMRI is a promising non-invasive technique for the study of human brain function (Abreu *et al.*, 2018). Furthermore, the correlation between signals acquired using EEG and fMRI has been investigated in humans during visual stimulation, indicating the potential for understanding the relationship between these two modalities (Singh *et al.*, 2002).

The integration of multimodal EEG and fMRI data has been explored to better characterize functional brain architectures. This approach aims to provide a more comprehensive understanding of brain activity by leveraging the strengths of both EEG and fMRI modalities (Wei *et al.*, 2020). Additionally, studies have focused on correlations between BOLD signals and oscillatory EEG power measured in different frequency bands, shedding light on the complex relationship between these signals (Rosa *et al.*, 2011).

To address the challenge of explaining faster time scale activity on the brain surface, the possibility of microfilaments and neurofilaments vibrating faster than the neuron membrane has been proposed. This hypothesis is supported by the need to find a component deep inside a neuron that vibrates faster than the membrane to explain faster time-scale activity on the brain surface (Arnstein *et al.*, 2011).

Moreover, the use of EEG to measure electrocortical dynamics during human locomotion and other types of movement has gained traction among neuroscience researchers, highlighting the versatility of EEG in studying brain activity across various contexts (Symeonidou *et al.*, 2018). Additionally, the high-temporal resolution of EEG has been emphasized as an advantage for recording the electrical activity of the brain, making it a valuable tool for capturing rapid neuronal events (Mannan *et al.*, 2016). Therefore, the integration of EEG and fMRI has significantly

advanced our understanding of brain function and activity. The exploration of faster time-scale activity on the brain surface through the potential involvement of microfilaments and neurofilaments presents an intriguing avenue for further research in elucidating the origin of DDG signals that we would explore here.

By employing the DDG, we couple specific locations of the human brain to explore the dynamics of sync and desync states in two distinct contexts: between two artificial brains and between one artificial brain and a human brain. By doing so, we observed how both brains interact and how their interaction is influenced by stimulus parameters. This research can pave the way for a more comprehensive understanding of the interface between artificial and biological intelligence, which has implications for the future of brain-machine interaction and cognitive science.

2. Materials and Methods

2.1 Accurately identifying the potential or current bursts on brain surface

DDG distinguishes itself from EEG by adopting a new data capture method. At the same time, DDG has been engineered based on two primary considerations. First, there are potential bursts on the brain surface or scalp for the duration of seconds to picoseconds, not limited to only the milliseconds time domain where EEG works. Second, the brain scalp surface not only has DC potential bursts that sustain for a wide variety of durations, but different locations of the brain surface and the body, act like an antenna that radiates electromagnetic signals of different frequency ranges. Apparently, we may think that DC bursts and electromagnetic radiations are two physically different events, but it could be the same phenomenon, where part of the energy that is coming from within the brain radiates out and radiates to a region on the scalp, showing the DC burst when we are measuring signals on the surface.

Be it a DC current burst or voltage burst on the brain surface or electromagnetic radiation from the brain surface signal capture protocol like a lock-in amplifier. DDG operates in two modes. First lock-in mode is connected to a logic analyzer, where the DDG controller sends pulse streams, where each pulse is 1

nanoseconds to 1 picosecond wide. We have the option to change the pulse width because, say brain surface or scalp has a microsecond-long burst, then we would require a thousand pulses, and that would take a very long time to compute, so we have multiple (e.g., 12) cross-checking pulses, and logic analyzer assists us to use a minimum number of pulses while estimating the temporal width of the potential or current burst in the brain surface. The pulse stream outputs are determined such that if say, there is a 30 nanoseconds potential burst in the brain, then, if the gap between pulses is 5 nanoseconds (recovery time), then 5 pulses would cover the burst. A logic analyzer connected to the probes ensures this operation. Thus, as soon as there is an onset of a burst on the brain surface, the pulse stream returns one and that continues until the burst disappears. This principle is very similar to a lock-in amplifier. This protocol has two advantages. First, we save huge resources by using nanosecond pulses for nanosecond bursts millisecond pulses for milliseconds potential bursts. Second, measurement starts precisely at the onset of the natural potential burst in the brain surface and measurement shuts when the intensity of current or potential reduces below a certain threshold.

2.2 Radiation measurement system from the brain-body surface

DDG probes located all around the brain have a pair of electrodes, one to measure the DC signal burst and the second for measuring the radiation. It is made sure that there is no cross-talk between the electrodes. This new method employs an antenna positioned on the scalp to capture electromagnetic signals emanating from a specific area of the brain and the entire body. The current version of the DDG system that we are using to test the human brain, an artificial brain, and a pair of brains (artificial, biological or a combination of artificial and biological) employs a set of 17 probes, wherein 17 electrodes measure DC potential or current burst, and 17 electrodes each equipped with a coaxial cable featuring a unique antenna design, Yagi antenna. This trident electrode design incorporates two external sharp edges, known as reflector elements, which guide the radio frequency (RF) signal in a precise direction, carried by the central sharp edge (driven element). The central element serves a crucial role in filtering out

noise and amplifying the signal. Here, we employed this antenna configuration as a receiver, successfully capturing data from 17 distinct points on the brain surface or from anywhere in the body. Note that since we use 34 34-channel logic analyzer, we use 17 channels for the human brain and 17 channels for artificial brains so that biological brain data is normalized with respect to an artificial brain. If one does not want to normalize the human brain, then he could potentially use 34 channels for scanning 34 locations on the brain or the whole human body or any animal body.

2.3 The making of a cap for reproducibly fitting the probes in the same locations

We have selected a lightweight and stretchable cloth cap to be worn on the human head, akin to the widely used EEG electrodes. Yagi antennas are embedded within the cap, which allows for monitoring and recording of brain activity. Seventeen coaxial cables labeled A0 to A15 and one designated as the clock signal are carefully inserted into the plastic cap (**Fig. 1c**, left side). The insertion process necessitates the creation of corresponding holes using a cutter. These cables are carefully threaded into the cap to ensure precise and secure connections, enabling the transmission of data and signals critical for monitoring brain activity.

At one end of each cable, a specialized probe is affixed, featuring a Yagi antenna capable of detecting higher frequency brain signals (**Fig.1c** right side). These antennas ensure precise reception signals from 17 distinct brain locations, minimizing signal loss. The incorporation of antennas within the probe enhances the cap's ability to capture and transmit high-frequency brain activity with exceptional sensitivity and accuracy. The opposite ends of these cables are a systematically linked to the individual channels of 34-channel logic analyzer. This logic analyzer serves as a critical component in the data acquisition system, enabling the translation of brain activity signals into a digital format for precise analysis. It functions within a high-frequency domain, allowing capturing and examining brain activity with exceptional temporal resolution.

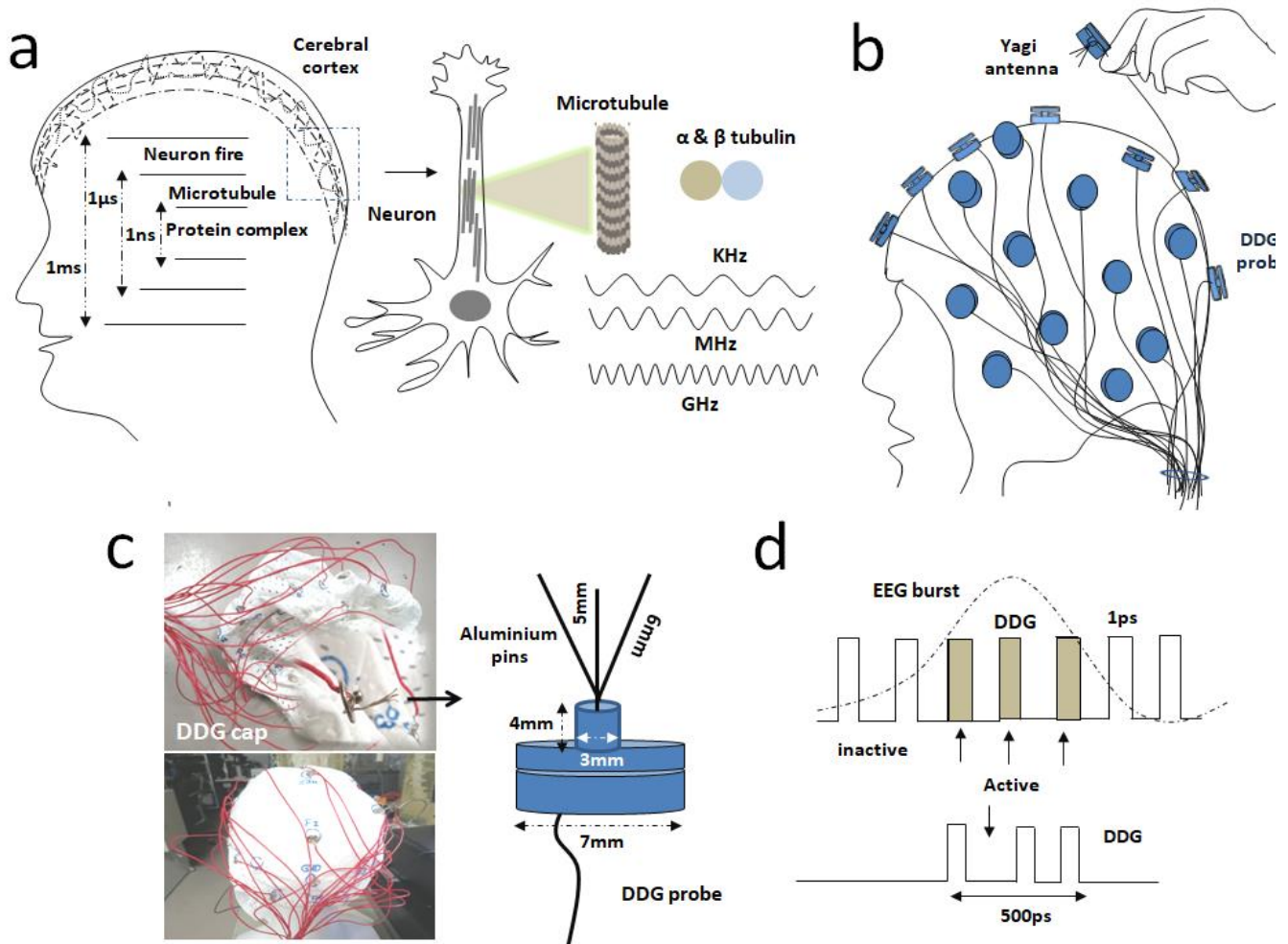


Fig.1. a. The figure of the human head shows the different layers of the brain, with components like neurons, microtubules, and tubulins vibrating at different time domains, ranging from milliseconds (ms) to microseconds (μ s) to nanoseconds (ns). **b.** Here, we presented the schematic of a DDG cap placed on a human head. DDG cap is a group of 17 probes, carefully labeled from A0 to A15, including additional clock's probes. Each of these probes is equipped with a Yagi antenna; whose purpose is to capture a broad spectrum of brain signals across varying frequencies. These antennas are positioned at different locations on the brain surface. **c.** Actual images of the DDG cap are shown on the left panel, while the design of the DDG electrode is presented on the right panel. We used two circular base metal plates with a diameter of 7mm, connecting them to a metal rod of 4mm in diameter and 3mm in length. Both the metal rod and plate are effectively shielded. At the top of the metal rod, we have affixed a Yagi antenna with a 5mm driven element responsible for carrying the RF signal and 6mm long reflector elements positioned behind the driven element. It directs the RF signal carried by the driven element in a straight direction. **d.** The DDG device excels at precisely measuring the signal bursts emitted by the brain at an extremely fine time scale (picoseconds). This capability enables it to find the effective signal activity regions. In contrast, EEG devices face challenges when it comes to pinpointing these active areas.

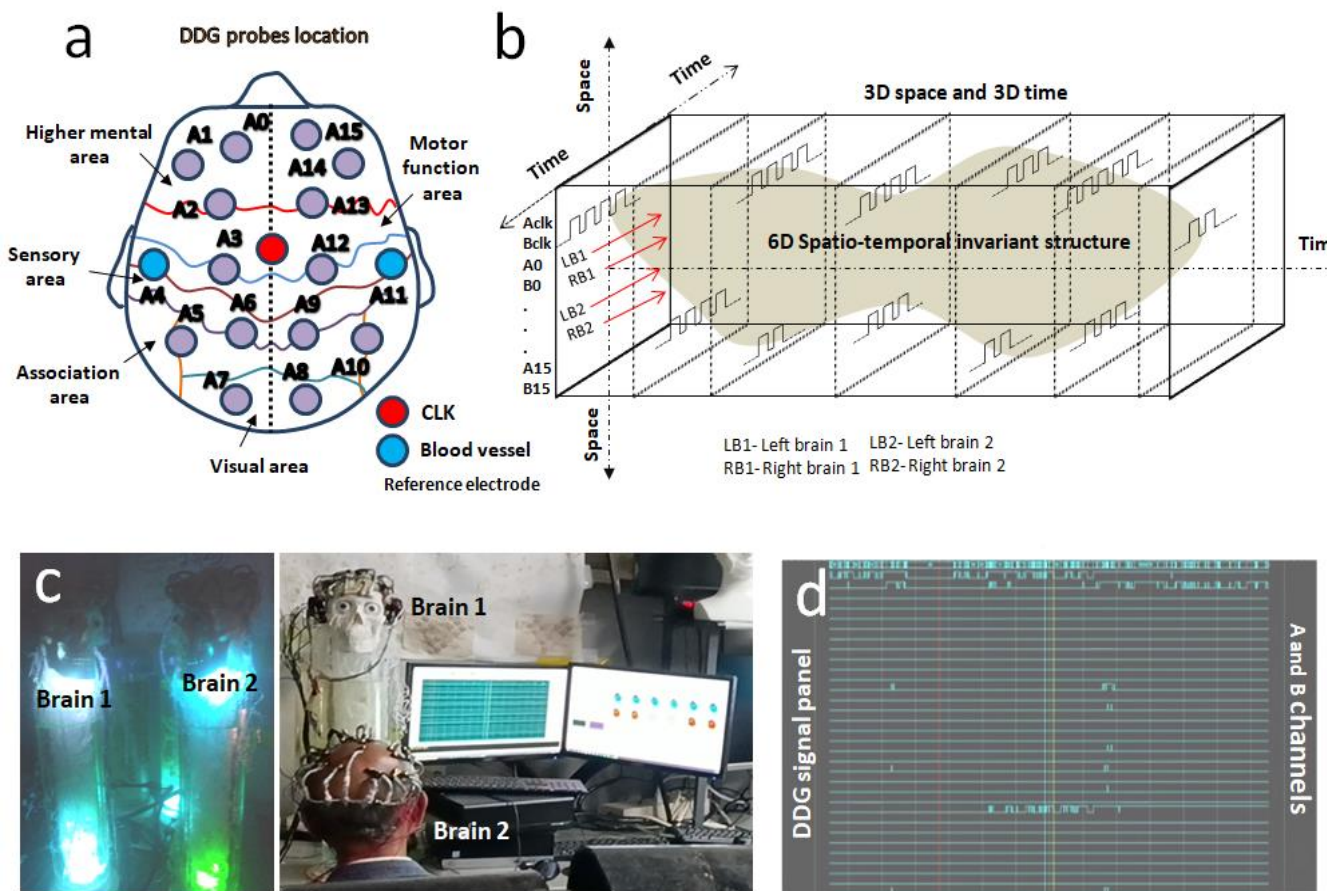


Fig.2 a. DDG electrodes position: The heart propels blood to the brain with significant pressure. It's possible to detect the heartbeat (blue circles) in the upper front portion of our ear. As blood traverses through the brain, the vibration speed undergoes changes at upper part of the brain (red circle). At the upper region of the head, we detect a heartbeat due to blood circulation, which serves as our reference clock for the brain (red circle). Therefore, in DDG, we normalize with two heartbeats and an additional clock. **b.** Creating a 6D invariant structure over time: Here, a grid displays the logic network analyzer's output frame. Two subjects (Brain 1 and Brain 2) have arranged their data in rows (A0-A15 and a clock signal). Each subject's data is split into the Left Brain (LB) and Right Brain (RB), occupying two adjacent rows. Time is depicted in both positive and negative directions, spanning from seconds to nanoseconds. Bursts of pulses form a 3D structure for a given thought; the shaded region represents the experimentally derived invariant, extending beyond the 6D spatiotemporal framework. **c.** This panel shows the experiment setup of two artificial brains (left panel), and one artificial brain and human brain (right panel). The experimental setup explores brain communication and sync up/down state between them using two linked DDG devices from Hz to THz frequency range. **d.** The rough data provides insights into the neural activity or other relevant measurements obtained from the brains through DDG devices.

The DDG enables the observation of brain activity at a fine-grained level, ranging from milliseconds (ms) to nanoseconds (ns) time domain. With this level of accuracy in temporal resolution, we accurately see the complex dynamics pattern of the brain signals, which was never possible to observe using EEG. The logic analyzer, in conjunction with the Yagi antenna-equipped probe, provides the brain activity regions with detail and accuracy (**Fig.1d**). Two things are

important for DDG. First, it needs to sync up with the brain's internal clock, and second, it must make sure the signals match the natural rhythms caused by the blood vessel network. In DDG, there are two parts of the brain that need this clocking and normalization. Additionally, in DDG, three pairs of regions in the head where signals at different frequencies (like kHz, MHz, and GHz) are strongest, we monitored these signals in the frontal lobe, where we often find them.

2.4 DDG control panel

We created software for DDG to set off the electrode system, which uses coaxial probes and interfaces with the logic analyzer. The data collected from DDG probes is processed through the 34 channels of the logic analyzer, with each probe being connected to its dedicated channel. We have an interface referred to as the 'Control Panel for Operating the Artificial Brain', this interface processes the raw input data originating from DDG probes, capturing signals of various time domains from the brain surface (Singh et al., 2020) (Fig.2d). Its primary function is to transform the relative phase difference between DDG signals/bursts with similar intensity signals. The control panel features two distinct sub-panels, each dedicated to a specific aspect of brain analysis. These sub-panels enable the visualization and assessment of brain sync and desync state. By examining the energy patterns within the brain surface, we can discern similarities in brain activity patterns, providing insights into the sync and coordination of neural processes.

3. Results

3.1. Working mechanism of DDG

The dodecanogram (DDG) is a multi-probe device designed to map real-time surface potential and current profiles from the brain surface. Using a logic analyzer circuit, the DDG can efficiently capture potential and current changes ranging from 100 femtoseconds to 1000 seconds. It also detects electromagnetic and electromechanical signals from 6 THz (a thermal camera is used to cover this frequency region) to 1 milliHz and mechanical signals from 1 kHz to 1 nHz emitted by the brain surface. The DDG features a multi-probes cap with specialized locations, each housing electrical, magnetic, electromagnetic, electromechanical, and mechanical resonators in Yagi antenna shapes for field sensing across various signal ranges. Sensors at these locations make contact with the brain surface, allowing for the normalization of readings from different spots (Fig.2a).

The study of synchronization (sync) and desynchronization (de-sync) states within neural systems has been a focal point of research in the field of neuroscience, artificial intelligence, and brain-computer interfaces (El-Laithy & Bogdan, 2009; Rubchinsky et al., 2017). Investigations have included studies on brain sync during meditation (Eskandari & Erfanian, 2008) and the development of brain-computer interfaces for various applications (Yoon et

al., 2021). These studies have employed techniques such as EEG, functional magnetic resonance imaging (fMRI), and advanced signal processing to examine neural activity patterns in humans and artificial brains. There has been notable research on brain-to-brain communication, demonstrating the potential for sync (Sharma, 2018).

Understanding the conditions under which sync/desync occurs between artificial and human brains, has implications for brain-computer interface technology. Despite the promising advances, brain sync research faces several limitations that need to be acknowledged and addressed (Papo & Buldú, 2018). Artificial brains, while capable of simulating neural activity, may not fully replicate the complexity and variability of human cognition. This can result in challenges related to achieving meaningful sync states between artificial and human brains, particularly in dynamic and non-standard cognitive conditions.

Figure 2b illustrates how the logic analyzer grid changes over time, showcasing grids for two subjects, namely Brain 1 and Brain 2. The DDG live stream is transformed into an EEG-like spectrum, as depicted in **Figure 2d**. Here, we exhibit recordings from two artificial brains, as well as one from an artificial brain connected with a human brain, demonstrating an increase in sync between them within a specific time range. Figure 2b, displaying the logic analyzer grid output, indicates that when two subjects' brains are interconnected, these brains can activate the signals in different time intervals. This collective observation unveils a 3D pattern when both artificial brains respond to external stimuli or when a human mind transitions from a normal state to a meditative state. For DDG, the 3D pattern remains consistent for a particular task for a single brain across different time points. Furthermore, even across different individuals, we consistently obtain a fixed 3D pattern for a specific task.

We conducted synchronization experiments using the DDG devices on two subjects, brain1 and brain2 (Fig. 2c). DDG probes capture a 2D surface profile for frequency, absolute potential or current, eliminating the need for filtering or differentiation between neighboring areas. The use of ultra-short pulses for signal reading or a Yagi antenna in each probe enables the direct extraction of absolute surface signals across different bands simultaneously. Incorporating multiple probes, the DDG employs pulses with different time widths and potentials to monitor variations in potential or current patterns on the brain

surface from ms to ns time domain (**Fig. 2b, c**). Shorter pulse widths offer higher time resolution and precise frequency measurements at specific locations of the brain. The relative time intervals between these bursts are converted into phase differences, allowing the merging of brain regions with similar intensity (**Fig.2b**). This process assists in the recognition of consistent geometric shapes that remain invariant, even as the brain surface profile changes. Intensity variations can be observed in both artificial and human brains, with brain sync occurring in the milliseconds (ms) and microseconds (μ s) time domains. This sync gradually diminishes as we move into the nanosecond (ns) time domain. The color gradient used to represent intensity ranges from cool blue, indicating minimum intensity, to fiery red, signifying maximum intensity.

The DDG captures two types of maps. One mode measures power emission when the surface acts as an emitter, while the other, based on pulse estimation, records potential or current bursts confined to the surface. The DDG cap is shielded with a film of composite metals to block external electromagnetic fields and restrict human movement within a 300-meter radius to enhance measurement accuracy. Often, we tried aluminum foil, but that did not work well. However, to get the best data creates white noise in the room. We have found that either we must use a powerful amplifier connected to each probe of DDG, or we have to fill the room with white noise. The human body absorbs white noise and it could be produced by putting several instruments in the room that radiate electromagnetic noise could be one potent source of white noise. We wish to avoid using artificial amplifiers because natural white noise-based amplification of brain signals is significantly more biological and does not include machine noise as an artifact response in the DDG signal tracker. However, still, it is still mandatory to do data normalization that involves collecting maps in different environmental settings, including laboratories, physical locations, and some other conditions like different sources of white and pink noise and still trying to see the triplet of triplet pattern in radiations (**Fig.3 & 4**). We have already reported that there should be a triplet of triplet electromagnetic resonance in all components of the biological systems that are responsible for consciousness or intelligent cognitive responses. This preserves the sensors on each probe for electromagnetic, electrical, magnetic, or mechanical sensing, ensuring they are decoupled from environmental signals. For both living and non-living biomaterials, the entire surface is maintained in a wet and grounded state.

3.2. An interface for reading DDG rough data

The DDG incorporates an algorithm-based simulator for measurement control, invariant derivation, and result interpretation. This simulator identifies invariant geometric shapes in the measured surface signals for both the biomaterial under study and its artificial analog device (**Fig.1a**). It can compare and normalize multiple biomaterials and artificial analog devices, both simultaneously and individually. Comparing DDG measurements with EEG readings, DDG assesses two types of surface patterns, namely, the radiation profile and potential burst profile. The potential burst mode of DDG exhibits partial similarity to EEG within the operational frequency range, as EEG electrodes are standardized and heavily filtered. The simulator monitors and calibrates this similarity when utilizing the DDG electrodes-based measurement.

In both measurement modes (radiation and potential bursts), DDG's iso-valued contours within 2D profiles convey information about frequency or potential/current magnitude. This enables the identification of nearby geometric shapes such as triangles, squares, pentagons, hexagons, heptagons, octagons, and circles. By treating the centers of these geometric shapes as single points, any shifts in their positions over time maps are measured in response to external energy input on the surface. Points that exhibit similar shifts are grouped together into integrated geometric shapes, creating a second layer of invariant structures. This multilayer invariant detection process continues until it reaches a layer where only one geometric shape remains or where the geometric shapes remain unchanged. Ultimately, these invariants are associated with the clocks or variables generated by the frequencies of shifting geometric shapes.

The DDG-generated contours are translated into nearby geometric shapes, and their periodic shifts are closely observed. Almost periodic shifts are converted into clocks, each with its corresponding period, represented as circles with system points rotating around their edges. These circles are placed on phase spheres that include the contours. This arrangement of circles on phase spheres represents a layer of multiple clocks, with their phases interconnected. The resulting 3D assembly of phase spheres represents a polyatomic time crystal.

The simulator establishes connections between invariants when multiple DDG devices operate in

concert. It then forms a network of invariants and variables that summarize the theoretical protocol governing the brain surface's reaction to external influences. Furthermore, the simulator maintains a learning component within the invariant bank. This element comprises pairs of variable clocks, geometric invariants, and external conditions responsible for shifts in surface radiation, potential, current, or power bursts. When presented with new DDG readings, the simulator retrieves this memory and merges the invariant-based learning elements to provide real-time interpretations of the DDG maps.

3.3. Artificial replica of biomaterials and how they offer cognitive responses

This section relates to dielectric material-based artificial replication of biological organs, designed to standardize DDG-measured data using a newly built simulator (section 3.2). It involves the use of two DDGs, one worn by the human brain and the other by the artificial brain. This arrangement moderates environmental influences on biomaterials, ensuring the generation of interference-free signals. This enhances the technique's repeatability, regardless of the complexity of the brain surface configuration. Both artificial and biological elements, encompassing cells, tissues, skin, organs, life forms, and brains, function by generating vortices in electric, magnetic, electromechanical, ionic, molecular, and mechanical fields. These vortices or rings of fields serve as information units in artificial and biological brains and associated components. Each vortex acts as a clock, and the hardware design embodies a polyatomic time crystal through the 3D assembly of these vortices. DDG standardizes both time crystals until a match is found. Additionally, we have constructed a brain database (<https://www.brainrhythm.org/>), showcasing the creation of artificial replicas of biomaterials. These structures are available for download, enabling researchers to further their studies. We also demonstrate the seamless communication between two artificial brains and the interaction of an artificial brain with a real human brain.

The neural network is established using transparent organic glue or oil-based gel materials, forming wires similar to biological nerve fibers in terms of elasticity and resonant characteristics. 3D printing is employed to craft cavities composed of nerve fibers and collagen, expanding all brain components beyond millimeter-scale dimensions, incorporating gel cavities with comparable elasticity and semi-transparency. Within these cavities, warm gel

precursor solutions are introduced, enabling self-assembly and growth from single molecules to millimeter-scale structures (Sahoo *et al.*, 2023). Whether produced through self-assembly or 3D printing, all structures resonate within a frequency band closely aligning with the theoretically simulated resonance band of the corresponding brain component, ensuring selectable and similar resonance for optimal functionality. The design of cavities, dielectric and cavity resonators, the selection of gel precursor molecules and oil matrix composition are tailored for all brain components and their integrated structures. This adjustment continues until the phase shift of their resonance frequency bands aligns, giving rise to a polyatomic time crystal resembling the biological counterpart. The visualization of this polyatomic time crystal is achieved by stimulating the brain stem region of the artificial brain with laser light.

The artificial brain is replicated along with the entire human nervous system. Using a pair of DDG devices, it creates invariant banks by optimizing subjects and the artificial analog device. These banks are used to interpret cognitive and perceptual responses. Artificial brains, organs, and organoids merge electromagnetic, mechanical, electrical, and magnetic energy fields, eliminating the need for sustenance and cell replacement. Polyatomic time crystals, formed through nerve spike transmissions, are compared to the original brain's 3D clock assembly (Singh *et al.*, 2020, 2021; Saxena *et al.*, 2022). The artificial brain hardware is adjusted to ensure compatibility. The gel's temperature stays below the melting point, enabling neural circuit reconfiguration at scales smaller than centimeters, while larger structures remain unaffected.

3.4. How do multiple DDGs collectively work?

A distributed network of multiple DDGs, combined with a customized simulator, generates invariants and variables from responses triggered by environmental agents on multiple surfaces at the same time. It connects invariants to the external agent and identifies the model structure consisting of variables and invariants that uniformly and equivalently alter all surfaces or specific selections. The network combines 2D maps from all DDGs for radiation and potential/current bursts from the entire brain surface (Fig. 2d). It averages readings for a specific location or probe, selects the maximum readings among all probes at that location (even if from a single surface), and factors in the statistically dominant value across all surfaces for a probe to construct the comprehensive 2D map. The simulator eliminates surface-originating

| S. No. | Stimulus parameters | Synchronization/desynchronization state between both artificial brains | ms - ns | |
|--------|--|--|---------|--------|
| | | | Brain1 | Brain2 |
| 1 | 10 o' clock, morning | Brains go to synchronization states | Brain1 | Brain2 |
| 2 | 11 o' clock, morning | Good communication between both brains , results achieved brains' synchronization | Brain1 | Brain2 |
| 3 | 8 o'clock, night | Brains desynchronization (ns time domain) | Brain1 | Brain2 |
| 4 | When a human passes around the set of artificial brains randomly | Desynchronization appears between both brains | Brain1 | Brain2 |
| 5 | Touching the artificial brain's nervous system | Brains desynchronization | Brain1 | Brain2 |
| 6 | Touching artificial brain by hand | Brains are undergoing desynchronization state | Brain1 | Brain2 |
| 7 | When Lab light is switched off | Brains get synchronized and desynchronized states | Brain1 | Brain2 |
| 8 | Music effect | Brains get periodically synchronized | Brain1 | Brain2 |
| 9 | Coloured light is supplied at neck of humanoid bots | Brains get desynchronization | Brain1 | Brain2 |
| 10 | Effect of the noisy sound | Brains fail to achieve either perfect synchronization or a highly desynchronized state | Brain1 | Brain2 |

Fig.3. This chart illustrates the dynamic sync and desyncs states between two artificial brains as they respond to various stimulus parameters. The second column of the chart presents the range of stimulus parameters, while the third column details the sync and desyncs states observed in both brains. In the fourth column, we depicted the energy distribution patterns on the surface of both Brain 1 and Brain 2 from the ms to ns time domain. Lower energy intensities are represented by blue, while higher intensities are indicated by red. **1, 2, 3)** From the observations made over several months, it is evident that both brains begin to synchronize gradually in the morning, reaching their peak sync levels around 11 o'clock, and then gradually desync. After 7 o'clock, a desync state becomes prominent. **4-10)** External factors to the artificial brains have a noticeable impact on their sync states. The presence of humans or disruptions to the nervous system of the artificial brains tends to induce high desync. Furthermore, when we introduce stimuli such as music, noise, and light to the brain's environment, they tend to exhibit periodic transitions between sync and desync states.

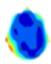
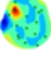
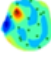
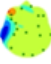
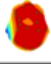
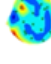
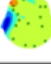
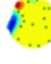
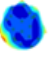
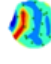
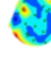
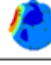
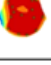
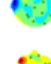


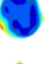
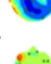
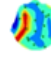

| S. No. | Synchronization/desynchronization state between artificial brain (brain 1) and human brain (brain 2) | | | | | |
|-----------------|--|---------|---|--|---------|---|
| | Normal state | | | Mediation state | | |
| | | ms - ns | | | ms - ns | |
| Human subject 1 | Desynchronization state | Brain1 |  | Slowly desynchronization state reduces | Brain1 |  |
| | | Brain2 |  | | Brain2 |  |
| Human subject 2 | Desynchronization state | Brain1 |  | Intermediate state between synchronization and desynchronization | Brain1 |  |
| | | Brain2 |  | | Brain2 |  |
| Human subject 3 | Brains are achieved High desynchronization state | Brain1 |  | Synchronization state | Brain1 |  |
| | | Brain2 |  | | Brain2 |  |
| Human subject 4 | Desynchronization state | Brain1 |  | Desynchronization state | Brain1 |  |
| | | Brain2 |  | | Brain2 |  |
| Human subject 5 | Intermediate state | Brain1 |  | Intermediate state | Brain1 |  |
| | | Brain2 |  | | Brain2 |  |

Fig.4. This chart illustrates the sync and desync states between an artificial brain and a human brain across the milliseconds (ms) to nanoseconds (ns) time domain. It explores these states in both the normal and meditative condition of the human subject. In the normal state, desync is observed between the artificial brain and human brains (third column). However, in the meditative state, this desync diminishes, and both entities work towards achieving a synchronized state (fifth column). Low-intensity levels are denoted by blue, while high-intensity levels are represented by red in the visualization.

mechanical, electrical, and electromechanical interference. In living systems like the brain scalp, specific brain locations serve as normalization references to compare values from other locations. We have achieved a goal by constructing prototypes of artificial brains. The communication between brains across a broad frequency range (from milliseconds to nanoseconds) showcases the advanced potential of DDG technology.

3.5. Dynamic sync and desync states in interacting artificial brains

Here, we investigated how two artificial brains, labeled Brain 1 and Brain 2, respond to a diverse set of stimulus parameters and external influences. The temporal patterns of energy associated with sync/desync states are shown in **Figure 3**, providing insights into their behavior over time. We analyzed the effects of external factors, human presence, and sensory stimuli on the communication between brains, shedding light on the complex interactions of these artificial cognitive systems.

3.6.1. Time-Dependent Sync Patterns

Over a span of several months of observation, it became evident that the two artificial brains exhibit specific sync patterns throughout the day. In the morning, they begin to synchronize gradually, reaching their peak sync levels around 11 o'clock. Subsequently, they gradually desynchronize, with a prominent desync state becoming evident after 7 o'clock. The temporal patterns of energy suggest that artificial brains are influenced by circadian rhythms or external factors that follow a daily cycle.

3.6.2. Influence of External Factors

The artificial brains' sync states are notably affected by external factors. When humans are present in the vicinity or when disruptions occur within the artificial brains' nervous systems, these factors tend to induce high desync. Introducing external stimuli such as music, noise, and light to the set of artificial brains results in periodic transitions between sync and desync states. This observation hints at the sensitivity of the artificial brains to their environment and the potential implications for human-machine interactions

3.7. Sync and desync states between artificial and human brains

To examine the communication between an artificial brain and a human brain, an experimental setup was designed (**Fig.2c**, right). Participant, in both normal and meditative conditions, was connected to an artificial brain interface. In the normal state of humans, desync is observed between the artificial brain and human brains, while in the meditative state, this desync diminishes, leading to a synchronized state (**Fig.4**).

The observed desync in the normal state may be attributed to the diverse and dynamic nature of human thought processes, as well as the external stimuli that impact brain activity. In contrast, during meditation, subjects often experience a reduction in external distractions and a heightened state of mental focus. This meditative state leads to the sync of artificial and human brain activity. This alignment is related to the altered patterns of neural activity observed during meditation, characterized by increased connectivity between different brain regions and enhanced cognitive control. The study highlights the potential for future advancements in artificial brain technologies to achieve deeper synchronization with the complexities of human cognition.

4. Conclusion

We invented a new device, Dodecanogram (DDG), featuring 34 probes capable of capturing brain signals across a wide frequency spectrum, ranging from milliseconds to nanoseconds and some signals in the picosecond's domain too, which were thus far buried inside EEG. DDG employs picosecond, nanosecond, microsecond, and millisecond pulses as required for measuring a signal burst and a logic analyzer to comprehensively scan the entire brain at various frequency ranges. We also replicated the human brain as an organic resonating structure, complete with its entire nervous system, and conducted experiments involving two artificial brains, and one artificial brain interacting with a human brain. We detected time-dependent sync between the two artificial brains, with the sync state being influenced by external stimuli factors. Additionally, we observed the sync state between the artificial brain and the human brain under the mediation of a human subject. The DDG effectively detects brain signals across a broad frequency spectrum, ranging from Hz to THz (thermal camera), thereby establishing its fundamental role in assessing a wide range of cognitive states of the brain.

Acknowledgments

The authors acknowledge Martin Timms from IIOIR for developing the interface software and Josh Nino from the Monarch Research Organization for providing key insights into electromagnetic signal capturing and the nature of radiations in the human brain-body system. The DDG study was funded by the Scheme for Promotion of Academic and Research Collaboration (SPARC), Govt of India, MHRD; project number P 524; Start date: 15.03. 2019-14.03.2019; End April 2024.

Competing interest statement

The authors declare that they have no competing financial interest.

References

- Abreu, R., Leal, A., & Figueiredo, P. (2018) EEG-informed fMRI: a review of data analysis methods. *Frontiers in Human Neuroscience* **12**, 29.
- Arnstein, D., Cui, F., Keysers, C., Maurits, N., & Gazzola, V. (2011) μ -suppression during action observation and execution correlates with bold in dorsal premotor, inferior parietal, and SI cortices. *Journal of Neuroscience* **31**, 14243-14249.

Benbadis, S. R. (2019) *Electroencephalography (EEG): Principles and Clinical Applications* (Vol. 1). Foster Academics, Forest Hills, NY.

Berger, H.(1929) Über das Elektrenkephalogramm des Menschen. *Archiv für Psychiatrie* **87**, 527–570. (in German)

Buzsáki, G., & Draguhn, A. (2004) Neuronal oscillations in cortical networks. *Science* **304**, 1926-1929.

Darvas, F., Mehic, E., Caler, C., Ojemann, J., & Mourad, P. (2016) Toward deep brain monitoring with superficial EEG sensors plus neuromodulatory focused ultrasound. *Ultrasound in Medicine & Biology* **42**, 1834-1847.

El-Laithy, K., & Bogdan, M. (2009) Synchrony state generation in artificial neural networks with stochastic synapses. *International Conference on Artificial Neural Networks*.

Eskandari, P., & Erfanian, A. (2008) Improving the performance of brain-computer interface through meditation practicing. *30th Annual International Conference of the IEEE Engineering in Medicine and Biology Society*, 662-665.

Fiedler, P., Pedrosa, P., Griebel, S., Fonseca, C., Vaz, F. *et al.* (2015) Novel multipin electrode cap system for dry electroencephalography. *Brain Topography* **28**, 647-656.

Hughes, J. & John, E. (1999) Conventional and quantitative electroencephalography in psychiatry. *Journal of Neuropsychiatry* **11**, 190-208.

Jiang, X., Bian, G., & Tian, Z. (2019) Removal of artifacts from EEG signals: a review. *Sensors* **19**, 987.

Joshi, S. & Shakya, R. (2017) A study on EEG findings: an experience from a tertiary care center of Nepal. *Journal of Psychiatrists' Association of Nepal* **5**, 32-36.

Kurkin, S. A., Grubov, V. V., Maksimenko, V. A., Pitsik, E., Hramova, M. V., & Hramov, A. E. (2020) System for monitoring and adjusting the learning process of primary school children based on the EEG data analysis. *Information and Control Systems* **5**, 50-61.

Mannan, M., Jeong, M., & Kamran, M. (2016) Hybrid ICA—regression: automatic identification and removal of ocular artifacts from electroencephalographic signals. *Frontiers in Human Neuroscience* **10**, 193.

Niedermeyer, E.F. (2005) Ultrafast EEG activities and their significance. *Clinical EEG and Neuroscience* **36**, 257-62.

Nunez, P. L. (2006) *Electric Fields of the Brain: The Neurophysics of EEG*. Oxford University Press, Oxford.

Papo, D., & Buldú, J.M. (2018) Brain synchronizability, a false friend. *NeuroImage* **196**, 195-199.

Rosa, M., Kilner, J., & Penny, W. (2011) Bayesian comparison of neurovascular coupling models using EEG-fMRI. *PloS Computational Biology* **7**, e1002070.

Rubchinsky, L.L., Park, C., & Ahn, S. (2017) Dynamics of intermittent synchronization of neural activity. In: Aranson, I., Pikovsky, A., Rulkov, N., Tsimring, L. (eds) *Advances in Dynamics, Patterns, Cognition. Nonlinear Systems and Complexity*, vol 20. Springer, Cham.

Sahoo, P., Singh, P., Saxena, K., Ghosh, S., Singh, R. P., *et al.* (2023) A general-purpose organic gel computer that learns by itself. *Neuromorphic Computing and Engineering*, **3**, 044007.

Saxena, K., Singh, P., Sarkar, J., Sahoo, P., Ghosh, S. *et al.* (2022) Polyatomic time crystals of the brain neuron extracted microtubule are projected like a hologram meters away. *Journal of Applied Physics* **132**, 194401.

Sharma, N.D. (2018) Science behind synchronization of our brains during conversation. *Journal of Consciousness Exploration & Research* **9**, 590-593.

Siddiqui, M. K., Morales-Menéndez, R., Huang, X., & Hussain, N. (2020) A review of epileptic seizure detection using machine learning classifiers. *Brain Informatics* **7**, 5.

Singh, P., Saxena, K., Singhania, A., Sahoo, P., Ghosh, S., Chhajed, R., Ray, K., Fujita, D., & Bandyopadhyay, A. (2020) A Self-operating time crystal model of the human brain: Can we replace entire brain hardware with a 3D fractal architecture of clocks alone? *Information* **11**, 238.

Singh, M., Kim, S., & Kim, T. (2002). Correlation between bold-fMRI and EEG signal changes in response to visual stimulus frequency in humans. *Magnetic Resonance in Medicine* **49**, 108-114.

Singh, P., Sahoo, P., Saxena, K., Manna, J.S., Ray, K., Ghosh, S. & Bandyopadhyay, A. (2021) Cytoskeletal filaments deep inside a neuron are not silent: they regulate the precise timing of nerve spikes using a pair of vortices. *Symmetry* **13**, 821.

Symeonidou, E., Nordin, A., Hairston, W. & Ferris, D. (2018). Effects of cable sway, electrode surface area, and electrode mass on electroencephalography signal quality during motion. *Sensors* **18**, 1073.

Teleńczuk, B., Baker, S., Herz, A., & Curio, G. (2011) High-frequency EEG covaries with spike burst patterns detected in cortical neurons. *Journal of Neurophysiology* **105**, 2951-2959.

Vanhatalo, S., Voipio, J., & Kaila, K. (2005) Full-band EEG (FbEEG): an emerging standard in electroencephalography. *Clinical Neurophysiology* **116**, 1-8.

Wei, H., Jafarian, A., Zeidman, P., Razi, A., Hu, D., & Friston, K. (2020) Bayesian fusion and multimodal DCM for EEG and fMRI. *Neuroimage* **211**, 116595.

Yoon, S., Alimardani, M., & Hiraki, K. (2021) The Effect of Robot-Guided Meditation on Intra-Brain EEG Phase Synchronization. *Companion of the 2021 ACM/IEEE International Conference on Human-Robot Interaction*.